High throughput microscopy of mechanism-based reporters in druginduced liver injury

Hiemstra, S.W.

Chapter 6

Novel regulators of Nrf2 activation relevant for drug-induced liver injury identified by a RNAi-based high throughput microscopy screening

Steven Hiemstra[1], Marije Niemeijer[1], Bram Herpers[1], Ian Copple[2], Steven Wink[1] and Bob van de Water[1]

[1]Division of Toxicology, Leiden Academic Centre for Drug Research, Leiden University, Leiden, The Netherlands

[2]MRC Centre for Drug Safety Science, Department of Molecular and Clinical Pharmacology, University of Liverpool, Liverpool, United Kingdom

Manuscript in preparation

Abstract

The Nrf2 anti-oxidant response pathway is key in protecting cells against reactive oxygen species-mediated toxicity. Also, it has been shown to play a central role in the protection of hepatocytes in drug induced liver injury (DILI). So far, the entire signaling networks that control Nrf2 remains unclear. Here we performed an imaging-based siRNA screen targeting all individual kinases, phosphatases, transcription factors and ubiquitinases (in total 3027 genes). The effect on Nrf2 activation was monitored in HepG2 cells by the CDDO-me-induced expression of the BAC-GFP-Srxn1 reporter. Candidate Nrf2 pathway regulators that upon knock down enhanced (58 genes) or inhibit (19 genes) the CDDO-me-induced Srxn1-GFP upregulation were validated with four single siRNAs. Hits were further validated using either diethylmaleate, which also directly activates the Nrf2 pathway, as well as by three different drugs that have DILI liabilities and activate Nrf2 in human hepatocytes. Validated hits that remained effective under all conditions included already established Nrf2 regulators, e.g. Atf3, Brd4 and RXRA, as well as various numerous modulators, e.g. PRDM10, BRPF3, ZNF217 and FOXE3. Some novel candidates directly affected the stability of Nrf2, ensuring sustained activation of downstream targets. Importantly, knock down of candidate enhancers of Nrf2 signaling increased the susceptibility to xenobiotic-induced cytotoxicity, supporting their critical role in the physiological control of the antioxidant stress response and, hence, cell defense programs. Our results contribute to a comprehensive understanding of the signaling network that controls one of the most important adaptive stress response programs.

Introduction

Reactive oxygen species (ROS) are formed by the partial reduction of oxygen molecules. ROS are formed in our cells as a by-product of oxidative phosphorylation in the mitochondria, thus cells are continuously exposed to very low amounts of reactive oxygen species. A large variety of exogenous sources, such as xenobiotic compounds and their reactive metabolites, can introduce large amounts of ROS, which can damage nucleic acids, proteins and lipids[197]. ROS are associated with carcinogenesis[198], neurodegeneration[199] and aging[200]. When cells suffer from ROS accumulation oxidative stress occurs.

Vertebrates have evolved a highly conserved cellular defense mechanism to detoxify cells from oxidative stress. The central transcription factor in this defense mechanism is nuclear factor erythroid 2-related factor 2 (*NFE2L2*/Nrf2). Nrf2 regulates a network of cytoprotective enzymes which are able to detoxify the cell from oxidative stress[201]. Nrf2 is a basic leucine zipper (bZIP) belonging to the Cap-N-collar transcription factor family. Under unstressed conditions, Nrf2 is bound to Kelch-like ECH-associated protein 1 (*KEAP1*/Keap1) in the cytosol (Supplemental figure 1). A Keap1 homodimer is able to bind to the ^{29}DLG^{31} and ^{79}ETGE^{82} motifs on the Nrf2 protein[183]. Keap1 links Nrf2 to the Cul3-based E3-ubiquitin ligase complex which leads to

ubiquitination and subsequent proteasomal degradation[183]. When oxidative stress occurs, ROS are able to bind to cysteine residues on the Keap1 protein, leading to a conformational change in the Keap1-Nrf2 complex. Nrf2 is still bound to Keap1 by the ^{79}ETGE^{82} motif, but not with the ^{29}DLG^{31} motif making it impossible to be degraded. Newly assembled Nrf2 cannot be bound by Keap1, will accumulate in the cytoplasm and subsequently translocate to the nucleus. In the nucleus Nrf2 heterodimerizes with small masculoaoneurotic fibrosarcoma (MAFs) proteins facilitating the binding to the Anti-Response Element (ARE). Nrf2 will transcribe a wide variety of target genes including detoxifying enzymes: sulfiredoxin1 (Srxn1), NAD(P)H dehydrogenase (Nqo1) and Heme oxygenase (Hmox1); xenobiotic metabolizing enzymes and nuclear hormone receptor retinoid X receptor alpha (supplementary figure 1)[55,202].

Drug-Induced liver injury (DILI) is a major problem in drug development and the clinic. DILI is associated with oxidative stress and the activation of the Nrf2 pathway and various drugs that induce liver injury activate Nrf2[26,203]. Likewise the Nrf2 anti-oxidant response also plays an important protective role in drug-induced liver injury (DILI). Nrf2 has been known to be activated in acetaminophen-induced liver injury, facilitating a protective response[204,205]. In mice Nrf2 activation is shown to be essential in the protection against hepatotoxicity. When Nrf2 knock-out, wildtype and Keap1 knock-out mice are treated with hepatotoxicants, Nrf2 knock-out mice are more susceptible to a number of hepatotoxicants, demonstrating protection against liver toxicity by the Nrf2 pathway[56].

Drug-induced liver injury occurs typically in the most susceptible individuals. Susceptibility could arise from genetic impairments in critical adaptive stress response signaling including Nrf2 signaling. Therefore, full mechanistic understanding of the Nrf2 pathway activation is pivotal in complete understanding of mechanisms that underlie DILI-induced hepatotoxicity and individual susceptibility. Various factors have already been identified that modulate Nrf2 activation. During post translational modification, different kinases (PKC, PI3K/AKT, GSK3β and CK2) can facilitate Nrf2 phosphorylation leading to Nrf2 nuclear accumulation and subsequent target activation[206–208]. GSK3β plays an additional role as it is able to phosphorylate Fyn; Fyn subsequently translocates to the nucleus and phosphorylates nuclear Nrf2, thereby targeting it for nuclear export and proteasomal degradation[209]. Also in its transcriptional activity Nrf2 is modulated. Not only MAFs can form heterodimers with Nrf2, but also other factors have been recognized to be involved with Nrf2 activation at the transcriptional level. Activating transcription factor 4 (Atf4) may promote Nrf2 activation by binding to Nrf2 in the nucleus[210]. Other nuclear factors are able to inhibit Nrf2 activation: BTB and CNC homolog 1 (Bach1) and Nuclear factor kappaB1 (NFκB) can occupy the Nrf2 promotor region, thereby inhibiting the Nrf2 response[211,212]. In addition, several microRNAs are known to be involved in regulation of translation of Nrf2 and Keap1[207]. Finally, Nrf2 activation can be regulated by different binding partners of the Nrf2 protein. p21, a cyclin dependent kinase involved in the DNA damage response, can directly bind to Nrf2, thus conferring with Nrf2 activation[213]. Caveolin-1, a

scaffold protein involved in uptake of lipophilic compounds, is shown to regulate Nrf2 activation in a similar manner[214].

Although many factors that control Nrf2 signaling have been defined, a fully unbiased discovery of all signaling components that control the Nrf2 activity has not been performed. Here, we set out to perform a large RNAi-based screen to identify novel regulators of Nrf2 activation to gain full mechanistic understanding of Nrf2 activation. Our systematic screening efforts targeting all individual kinases, phosphatases, ubiquitinases and transcription factors, validation screening resulted 58 suppressors of Nrf2 activation and 19 activators of Nrf2 activation. We confirmed their role in unstimulated conditions and diethyl maleate (DEM) stimulation at different time points. In addition, we tested whether DILI relevant Nrf2 inducers azathioprine, acetaminophen and diclofenac showed the same effect upon knock down of the validated hits. Furthermore, we showed the importance of the hits in cell death onset, confirming that these factors are important in the balance between cell survival and cell death.

Material and methods

Chemicals and exposures

Diethyl maleate (DEM) was obtained from Sigma (Zwijndrecht, The Netherlands). CDDO-me was a kind gift from Dr. Michael Wong and Prof. Paul O'Neill, Dept. of Chemistry, University of Liverpool [215]. Acetaminophen and diclofenac were obtained within the MIP DILI consortium and azathioprine was a kind gift from Dr. Weida Tong, NCTR-FDA. All compounds were dissolved in DMSO except for acetaminophen (DMEM). Hoechst 33342 (Thermo Scientific, Leiden, The Netherlands) 200 ng/ml was used to stain nuclei of live cells prior to compound exposure.

Cell line

Human hepatoma cell line HepG2 was obtained from the American type tissue culture collection (ATCC, Wesel, Germany). HepG2 cells were cultured in phenol red free Dublecco's modified Eagles medium (DMEM) supplemented with 10% (v/v) fetal bovine serum (FBS), 25 U/ml penicillin and 25 µg streptomycin (PSA, Invitrogen).

HepG2 BAC-GFP reporter cell lines

Mouse *SRXN1*, human *NFE2L2*, *KEAP1*, *NQO1* and *HMOX1* were selected and tagged with enhanced green fluorescent protein (GFP) as described previously using the bacterial artificial chromosome recombineering technique (BAC)[152] and stably introduced into HepG2 cells by transfection and 500 µg/ml G-418 selection as reported previously[145]. Characterization for *NQO1* and *HMOX1* were performed in a similar way as described previously[145].

siRNA transfections

Transient knock-downs were achieved using siGENOME siRNA reagents (50 nM; Dharmacon ThermoFisherScientific, Landsmeer, The Netherlands). Single siRNAs were used for deconvolution screening. Smartpool mixes were used for all other experiments. HepG2 cells were transfected with INTERFERin^{TM} (Polyplus transfection, Leusden, The Netherlands). Deconvolution screening was performed using the Biomek FX liquid handling (Beckman Coulter, Woerden, The Netherlands). Negative control mock did not contain siRNA, only INTERFERin. Cells were incubated for 72 hours with siRNA before compounds treatment and/or microscopy.

Cell death

Propidium iodide (100 µM) and Annexin-V-Alexa633 labeled cells were added in exposure medium to stain necrotic and apoptotic cells.

Microscopy

GFP intensity levels of reporter cell lines were measured using a Nikon TiE2000 confocal laser microscope equipped with an automated stage, perfect focus system and live cell control to ensure 37°C and CO_2 conditions during imaging. Images were made with 20X objective (NA = 0.75, Violet Corrected), 1x zoom 3x3 stitched imaging. Lasers 405 nm (Hoechst 33342), 488 nm (GFP), 561 nm (Propidium Iodide) and 640 nm (Annexin-V-Alexa633) were used for detection.

Quantitative image analysis

Image quantification was performed with CellProfiler 2.1.1 (Broad Institute, Cambridge, USA), HDF5 (version 2.10.1), R (version 3.2.2) and R studio (version 0.97.551) as reported previously (Wink *et al*, manuscript in preparation). Based on the Hoechst 33342 nuclear staining image CellProfiler defines objects. Based on the GFP signal, a cytoplasm mask was determined. The mean GFP intensity values were calculated as mean pixel value per cell for each pixel underneath the cytoplasm mask.

Statistical analysis

For primary screening plates were normalized to plate average; z-scores were calculated by using the plate average. The average z-scores of at least two independent experiments were used; z-score threshold of 1,5 and -1,2 were used in hit selection. For deconvolution screening plates were normalized to at least eight mock control wells; z-scores were calculated independently per plate. Z-scores to determine whether the threshold was reached were based on three independent replicates; z-score thresholds of 1,5 and -1,2 were used. The smartpool and at least two single siRNA sequences had to exceed the threshold to be called a validated hit. Relative GFP intensity was calculated by dividing the GFP intensity of the treatments by the GFP intensity of mock. Signal of cell death stains propidium iodide and Annexin-V were masked

and used to look for overlap with nuclear masks. Overlapping nuclei were counted as dead cells. The fraction of dead cells was calculated dividing the dead cells by total amount of nuclei. For cell death measurement in the bar graphs fractions positive for propidium iodide and Annexin-V were added up.

Results

A robust RNAi based phenotypic screen to identify regulators of the Nrf2 response pathway

Previously, we have established a GFP reporter platform to enable to visualize the live cell dynamics of the Nrf2 stress response pathway using confocal microscopy[145,180]. We tagged Keap1 (upstream sensor), Nrf2 (transcription factor) and Srxn1 (target of Nrf2) with green fluorescent protein to follow different layers of Nrf2 activation. Here, we used Nrf2 GFP reporter system to gain full mechanistic understanding of Nrf2 activation. Therefore, we applied a robust RNAi based screen to identify regulators of the Nrf2 pathway. As read-out for the screen we chose Srxn1-GFP, as expression of Srxn1 reflects transcriptionally active Nrf2. To induce expression of Srxn1 we applied a very potent inducer of the Nrf2 pathway: CDDO-me (also known as bardoxolone methyl)[215,216]. Live cell imaging of Srxn1-GFP induced with a dose range of CDDO-me was performed to determine the optimal concentration and time point (data not shown). Exposure with 30 nM CDDO-me for seven hours was selected as the most optimal concentration, as this concentration/time combination showed optimal Srxn1-GFP expression allowing the detection of siRNA-mediated enhancement and reduction of Srxn1-GFP expression. CDDO-me was applied 72 hours after transfection with siRNAs. Automated live cell imaging, followed by quantitative image analysis was performed to determine the levels of induction of Srxn1-GFP. As a result, control treatments showed expected induction (siKEAP1) and reduction (siNFE2L2) (supplementary figure 2).

Novel suppressors and enhancers of Nrf2 signaling

Next we screened for modulators of Nrf2 signaling. We started with a primary screen targeting 3027 genes targeting most cell signaling components including transcription factors (1415), kinases (706), ubiquitinases (534), deubiquitinases (95), epigenetic regulators (134) and TNF receptor signaling (143). In primary screening the siRNAs were applied in a smartpool mix containing four different sequences targeting one gene. A z-score was calculated for all 3027 siRNA knock downs and ranked by z-score value (figure 1A). Hit selection for hits activating upon knock down (hereafter called suppressors) was set at a z-score threshold of 1,5. Hit selection z-score threshold for inhibiting hits upon knock down (hereafter called enhancers) was set at -1,2. These values were also just above the z-scores for siKEAP1 and siNFE2L2, respectively. These z-score thresholds resulted in 95 suppressors and 84 enhancers, in total 179

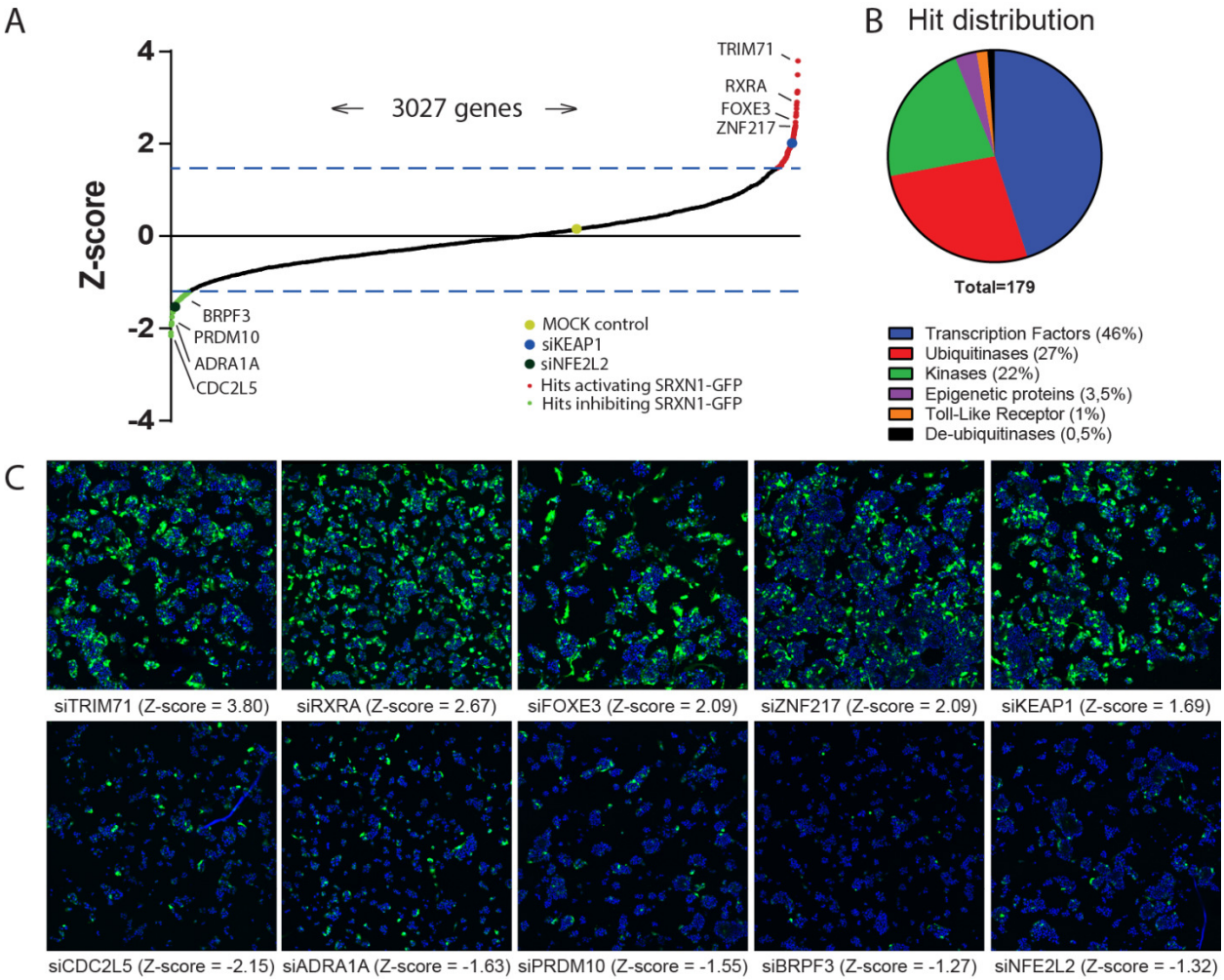

Figure 1: Primary screen identifies potential hits which are involved in Nrf2 activation. A) Z-score responses depicts the 3027 siRNA treatments on the x-axis and the corresponding z-score on the y-axis. Mock average is indicated in yellow, siKEAP1 in purple and siNFE2L2 in dark green. Activating hits selected for validation above z-score 1,5 indicated in red and inhibiting hits selected for validation below z-score -1,2 indicated in green. Z-scores are depicted as average of two independent replicates. B) Pie chard of the total hit distribution over the different protein families. C) Example images of suppressors (above) and of enhancers (below), including Keap1 and Nrf2 control.

hits. Interestingly, several suppressor hits exceeded activation of Keap1, among them siRXRA, siTRIM71, siZNF217 and siFOXE3. In addition, a subset of enhancers decrease Srxn1-GFP more than siNFE2L2, i.e. siCDC2L5, siADRA1A and siPRDM10. The three major libraries in the screen (transcription factors, kinases and ubiquitinases) were also highly represented in the observed hits, with a slight overrepresentation of ubiquitinases (figure 1B). Representative images of four top suppressors (siTRIM71, siRXRA, siFOXE3 and siZNF217), four top enhancers (siCDC2L5, siADRA1, siPRDM10 and siBRPF3) and Keap1 and Nrf2 controls showed clear enhancement or inhibition of the CDDO-me-induced Srxn1-GFP upregulation (figure 1C).

Next the different single siRNA sequences contained in the smartpool were tested to ensure

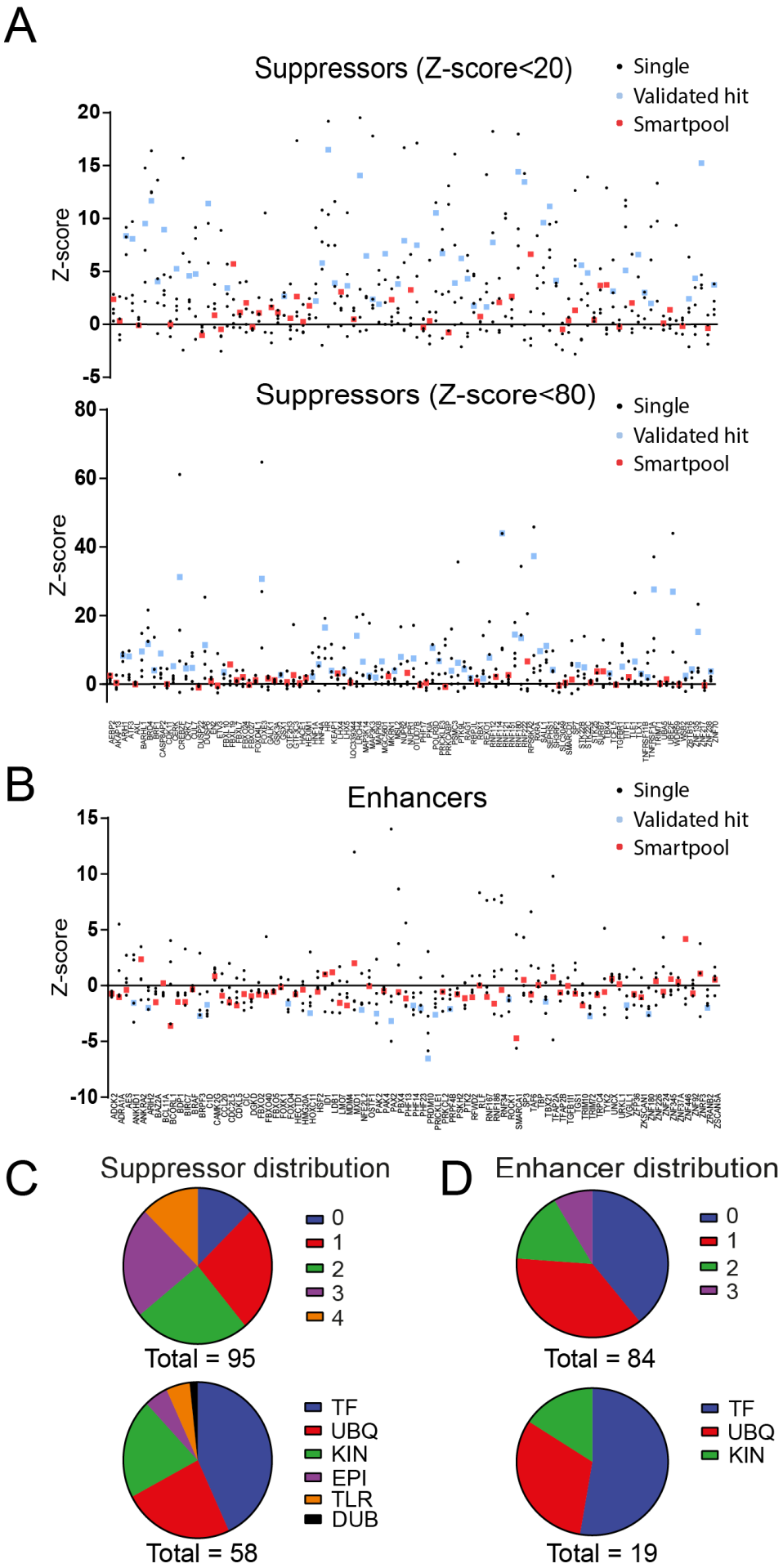

Figure 2: Deconvolution screen validates hits which are key modulators of Nrf2-mediated Srxn1 activation. A) The activating siRNA hits (suppressors) on the x-axis and the z-score on the y-axis. Each treatment shows a smartpool and four singles. Of a validated hit, the smartpool is indicated in blue, not validated hits are indicated in red. Z-score between -5 and 20 are depicted in the upper graph, z-scores from -5 to 80 are depicted in the lower graph. B) Same as A, but for inhibiting hits (enhancers), Z-scores depicted are between -10 and 15. C) Two pie charts: distribution of the activated hits showing the amount of single siRNA's validated (above) and distribution of the validated hits over the different siRNA gene libraries (below). D) Same as C, but for enhancers.

the effect of the smartpool mix was not an off-target effect of one of the single siRNAs. Smartpool mixes were incorporated in the deconvolution screen to assess reproducibility. For each siRNA treatment, z-scores were calculated for the smartpool and all four single siRNAs (figure 2A and 2B). For hit validation z-score thresholds of the primary screen were maintained. Hits were considered validated when at least two single siRNA sequences passed the threshold level. From the 95 suppressors 61% (58 hits) were considered as a validated hit. These 58 hits are representing all six gene families present in the screen (figure 2C). From the 84 enhancers 22.6% (19 hits) were considered as a validated hit. Only three gene families were present among these 19 hits (figure 2D).

Novel regulators modulate Nrf2 pathway independent of oxidative stress stimulus

Since the primary and deconvolution screen were performed with CDDO-me, we set out to confirm that the hits are either generic modulators of Nrf2 signaling or specific for CDDO-me. Therefore, first, we evaluated the effect of our candidates in control conditions; second, we evaluated all validated hits at an additional time point, 24 hours; and third, we used another Nrf2 activator diethyl maleate (DEM). First, we validated control activation of the pathway by testing siKEAP1, siNFE2L2 and untransfected control mock for all the conditions (figure 3A). All conditions showed reduced levels of Srxn1-GFP in siNFE2L2 and enhanced levels of Srxn1-GFP in siKEAP1 compared to mock. As expected, mean GFP intensity did differ between the conditions: not exposed mock conditions demonstrated baseline levels of Srxn1-GFP and 24 hours induction with DEM and CDDO-me resulted in higher induction compared to seven hours exposure. Next, we applied all validated hits and evaluated Srxn1-GFP after 72 hours of transfection without compound stimulation (figure 3B and 3C). Only two out of 58 suppressors did not show any increase without compound stimulation. siKeap1 had the largest increase compared to mock, followed by several strong hits siZNF217 and siFOXE3. Although baseline Srxn1-GFP levels were low, a reduction was visible for all 19 enhancers. siPRDM10, siBRPF3 and siPAX2 knock downs even demonstrated a stronger decrease than siNFE2L2. Secondly, when the stimulation with CDDO-me was prolonged until 24 hours, a similar pattern of activation for suppressing and enhancing hits was observed (figure 3B and C). The induction compared to mock for suppressing hits was less for 24 hours compared to seven hours. This is probably due to the higher Srxn1-GFP intensity in the untransfected mock control. Thirdly, stimulation with diethyl maleate (DEM) for 7 and 24 hours results in a similar pattern as CDDO-me (figure 3B and C). For both CDDO-me and DEM, siZNF217 and siFOXE3 showed an increase comparable to siKEAP1, indicating an important role for these genes in suppression of Nrf2 activation. In addition, siPRDM10 and siBRPF3 did exhibit a clear decrease throughout all conditions indicating a critical role in the enhancement of Nrf2 activation. Taken together, we conclude that our validated candidate genes regulate the Nrf2 response pathway in a generic way.

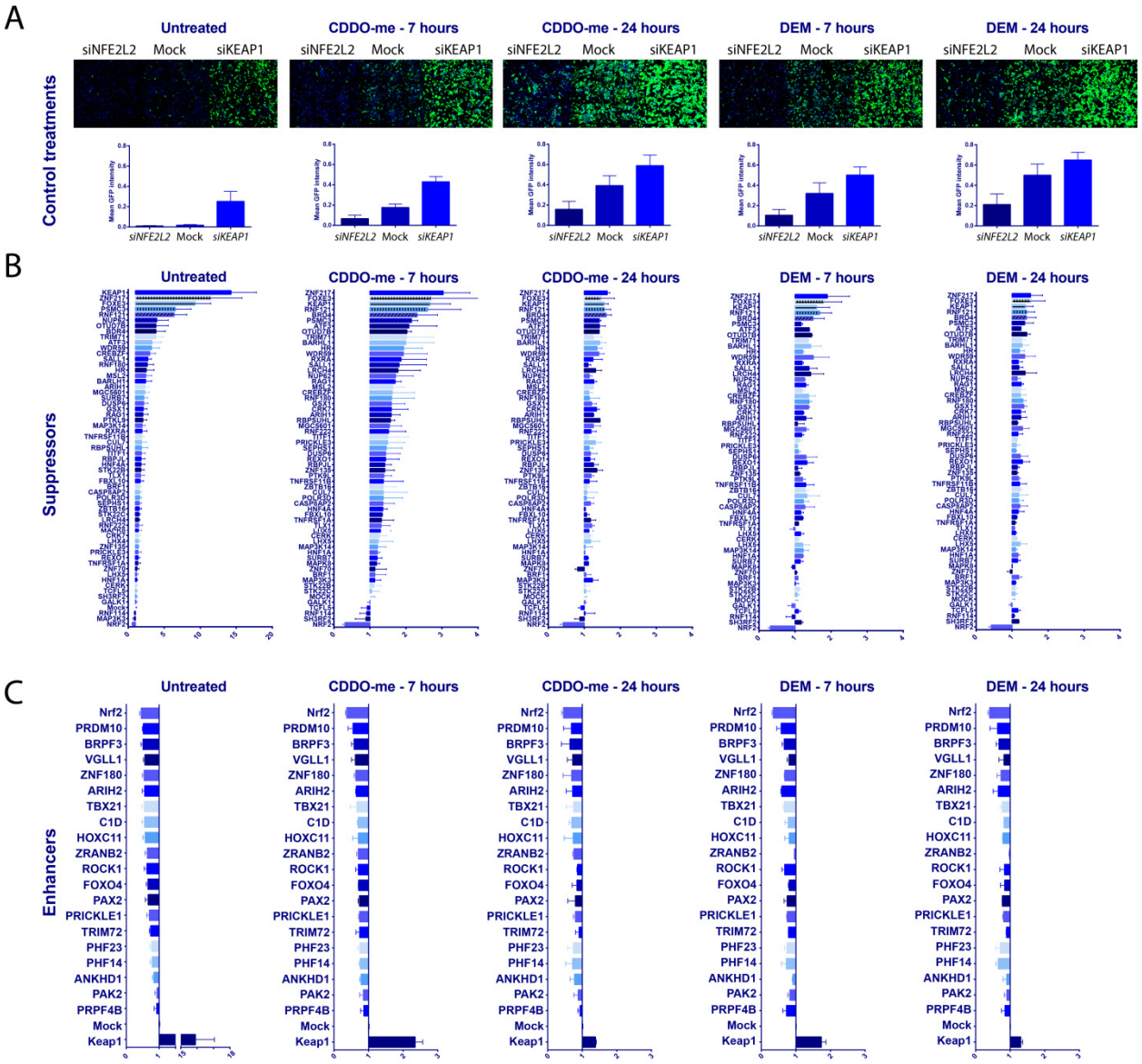

Figure 3: Hits also show activation/reduction of Nrf2 activation without stimulation, with 24 hours of CDDO-me and 7 and 24 hours of diethyl maleate (DEM). A) Representative images and quantified mean GFP intensity of Srxn1-GFP for siNFE2L2, mock and siKEAP1 for uninduced conditions, 30 nM CDDO-me 7 and 24 hours, 100 µM DEM for 7 hours and 24 hours. B) Relative GFP expression of suppressors without compound stimulation, with 7 or 24 hours of CDDO-me or DEM exposure. X-axis depicts GFP expression normalized to mock untransfected control. Y-axis shows all validated hits. C) Same graphs as in B, but for the enhancers.

Evaluation of GFP reporter cell lines of other target genes of Nrf2 after knock down with suppressors and enhancers

To investigate whether our validated hits were specific for Srxn1 activation or could activate the Nrf2 pathway in a broader sense, we constructed additional HepG2 BAC-GFP reporter cell lines for two other well studied downstream Nrf2 targets: Nqo1-GFP and Hmox1-GFP. Both Hmox1 and Nqo1 are often used as a read-out for Nrf2 signaling[217]. To validate Nrf2 dependency of the reporters we first performed knock down of Nrf2 and Keap1 in the Nqo1-GFP and Hmox1-GFP

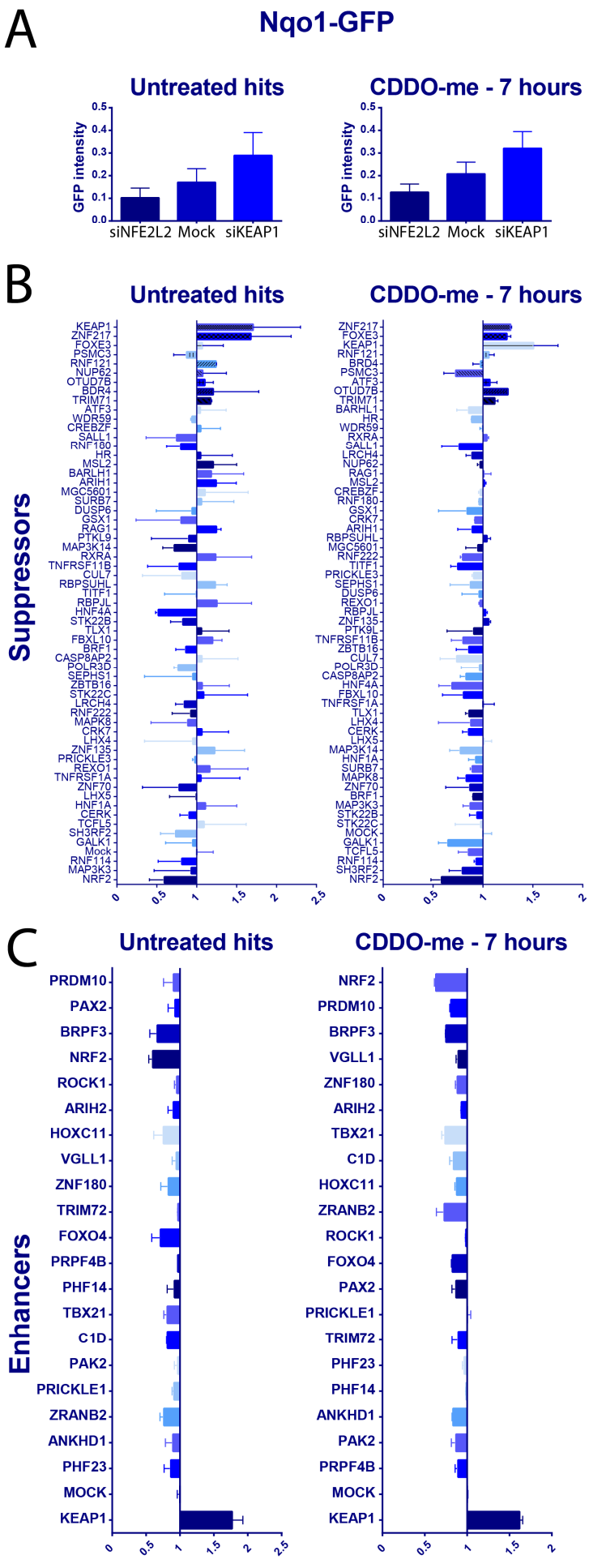

Figure 4. Effect of suppressors and enhancers on Nqo1-GFP expression. A) Mean GFP intensity of Nqo1-GFP for siNFE2L2, mock and siKEAP1 for untreated (left) and CDDO-me 30 nM for 7 hours (right). B) Relative GFP expression of suppressors in Nqo1-GFP. C) Relative GFP expression of enhancers in Nqo1-GFP.

cell lines (figure 4A and supplementary figure 3A). For both untreated and treated with seven hours of CDDO-me Nqo1 showed reduction after knock down of Nrf2 and showed upregulation after knock down of Keap1 (figure 4A). Hmox1 did not show Nrf2 dependency in untreated conditions and was also not upregulated by CDDO-me (data not shown); as an alternative used DEM, and DEM-induced Hmox1-GFP upregulation was dependent on Nrf2 (supplementary figure 3A). However, intriguingly, knock down of Keap1 did not increase, but also reduced Hmox1-GFP. Despite this inconsistence, we did evaluate the Hmox1-GFP further.

The strongest suppressors showed an upregulation of Nqo1-GFP either under basal conditions or CDDO-me conditions. Again siZNF217 and siFOXE3 exhibit clear increase in Nqo1-GFP compared to mock. In addition, also siTRIM71 and siRXRA showed an increase albeit less pronounced (figure 4B). Most enhancers showed a reduction of

Nqo1-GFP upon knock down, both in unstimulated and CDDO-me stimulated conditions (figure 4C). Overall, only a few suppressors and almost all enhancers demonstrated the expected effect in Nqo1-GFP. This difference is probably due to the high baseline expression of Nqo1-GFP, resulting in a small dynamic range to increase and a large dynamic range to decrease Nqo1-GFP. Hmox1-GFP displayed a more capricious pattern in all conditions for both suppressors and enhancers (supplementary figure 3B and C). Still, an increase in Hmox1-GFP was observed in siZNF217 and siTRIM71 after seven hours of DEM exposure and a decrease was observed in siBRPF3 after DEM treatment. The Nqo1-GFP support the notion that our candidate genes are involved the regulation of multiple Nrf2 target genes.

Candidate Nrf2 modulators modulate DILI compound-induced Nrf2 activation

Since Nrf2 signaling plays an important role in DILI, we were interested to see whether our validated candidate genes also modulate the Nrf2 acivation induced by drugs that have clinical DILI liabilities. Previously, we performed a large screen containing drugs to screen for stress response activation (Wink *et al*., manuscript in preparation). Based on this, we chose azathioprine, diclofenac and acetaminophen. First, we tested whether knock down of *NFE2L2* and *KEAP1* affected the Srxn1-GFP expression after drug treatment. A Nrf2-dependent activation of Srxn1-GFP was observed for all three drugs (figure 5A). Azathioprine demonstrated high levels of Srxn1-GFP induction in mock conditions compared to diclofenac and acetaminophen. Still, siKEAP1 increased expression of Srxn1-GFP upon azathioprine exposure. For both the suppressors and enhancers most knock downs led to a similar pattern compared to CDDO-me exposure (figure 5B and C). The differences were less pronounced in the suppressors for azathioprine, probably due to higher levels of Srxn1-GFP induction in mock conditions. Before mentioned candidate genes siZNF217, siFOXE3, siTRIM71, siRXRA, siPRDM10 and siBRPF3 again turned out as strongest modulators. Interestingly, suppressors ARIH1 and RBPSUHL showed for these drugs, especially acetaminophen and diclofenac, high induction compared to CDDO-me. This was confirmed by calculating the ratio between DILI drugs and unexposed control conditions for each knock down (supplementary figure 4). Altogether, this led us to the conclusion that our candidate genes are also relevant for the regulation of Nrf2 activation by DILI relevant drugs.

Candidates genes modulate the dynamics of Nrf2 and Keap1

Next we investigated whether our candidate genes affect the two most prominent regulators of Srxn1 activity: Nrf2 and Keap1. For this, we selected ten suppressors and ten enhancers. For the suppressors, we selected six highest ranked hits based on CDDO-me (7 hours) (figure 3B), except for BRD4, as BRD4 function in the Nrf2 pathway is already known. In addition, we included two hits, LRCH4 and RBPSUHL, which were strongly activated by the CDDO-me and DEM compared to untreated conditions (supplemental figure 4). Moreover, also MSL2 and

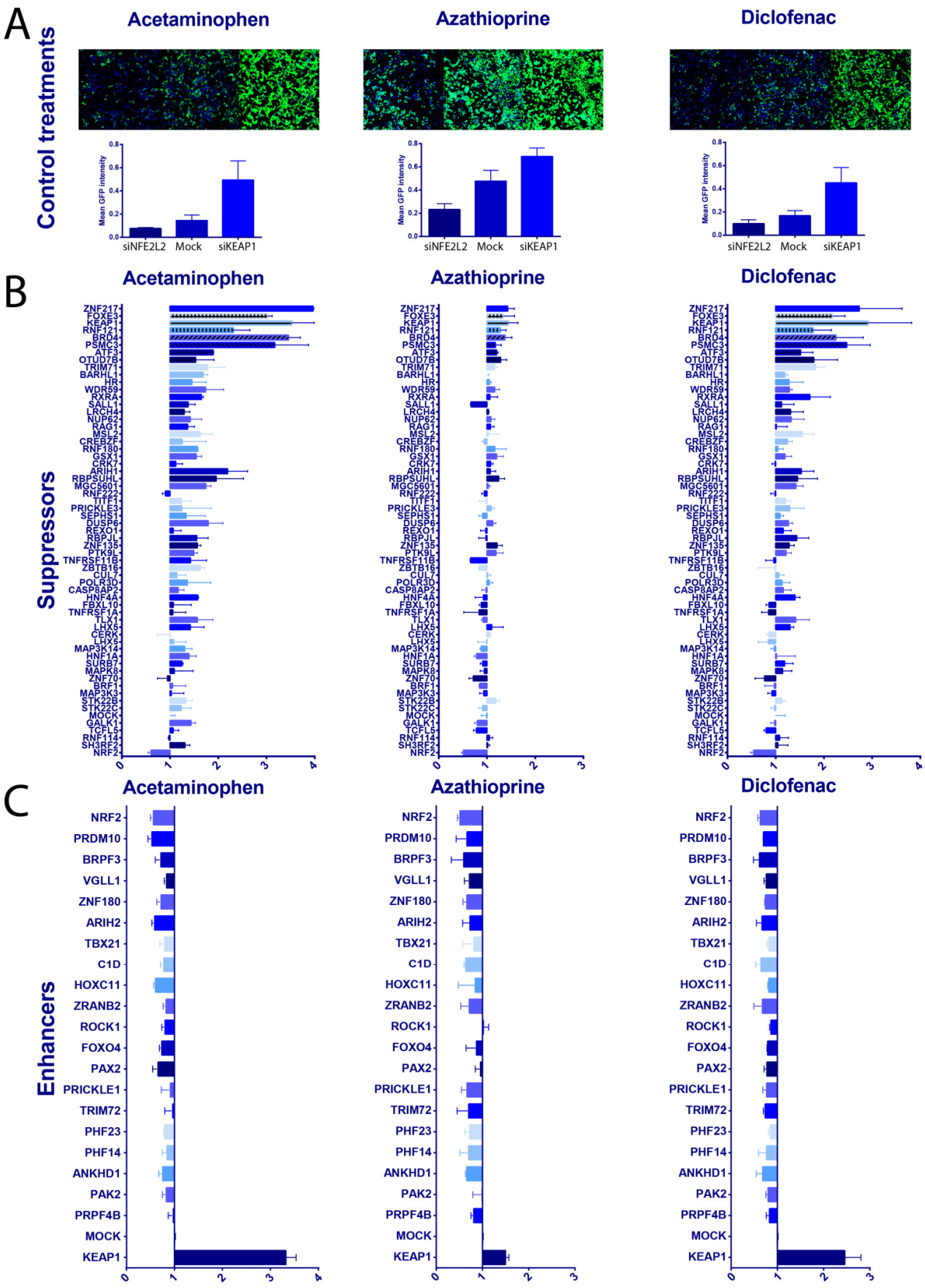
A
Acetaminophen
Azathioprine
Diclofenac
Control treatments
Mean GFP intensity
siNFE2L2
Mock
siKEAP1
B
Acetaminophen
Azathioprine
Diclofenac
Suppressors
C
Acetaminophen
Azathioprine
Diclofenac
Enhancers
NRF2
PRDM10
BRPF3
VGLL1
ZNF180
ARIH2
TBX21
C1D
HOXC11
ZRANB2
ROCK1
FOXO4
PAX2
PRICKLE1
TRIM72
PHF23
PHF14
ANKHD1
PAK2
PRPF4B
MOCK
KEAP1

Figure 5: Hits also show activation/reduction of Nrf2 activation after stimulation with drugs known to induce liver injury. A) Representative images and quantified mean GFP intensity of Srxn1-GFP for siNFE2L2, mock and siKEAP1 for acetaminophen (7.5 mM) (left), azathioprine (34 µM) (middle) and diclofenac 420 µM (right). B) Relative GFP expression of suppressors after stimulation with acetaminophen (left), azathioprine (middle) and diclofenac (right). X-axis depicts GFP expression normalized to mock untransfected control. Y-axis shows all validated hits. C) Same graphs as in B, but for the inhibiting hits.

ARIH1 were included, which strongly activated Srxn1-GFP for the three drugs inducing liver injury (supplemental figure 4). For the inhibiting hits upon knock down, we chose ten highest ranked hits based on CDDO-me seven hours treatment (figure 3C). To test the effect of the selected hits on upstream regulators Nrf2 and Keap1, we used previously characterized BAC-GFP reporters Nrf2-GFP and Keap1-GFP[49,145]. Nrf2-GFP and Keap1-GFP were transfected with the selected hits and subsequently exposed to CDDO-me and followed for 24 hours using automated live cell confocal microscopy. siPSMC3, siOTUD7B, siMSL2, siZNF217 and siRBPSUHL caused an increase in Nrf2-GFP levels compared to untransfected control (figure 6A). Interestingly, the ten enhancers showed a slight reduction of Nrf2-GFP accumulation in the nucleus compared to the untransfected control. For two hits, siC1D and siTBX21, this difference was more pronounced due to no increase in Nrf2-GFP accumulation upon CDDO-me exposure. This suggests C1D and TBX21 interfere with the Nrf2 accumulation and not at the level of target gene expression. All enhancers show a reduction of Keap1-GFP foci formation upon knock down, indicating a block of Keap1 degradation upon knock down (figure 6B). Seven suppressors, including siZNF217 and siFOXE3, resulted in increased Keap1-GFP foci formation. Remarkably, the three suppressors which do not increase Keap1-GFP foci formation upon knock down, PSMC3, OTUD7B and MSL2, were increasing Nrf2-GFP accumulation, thus this is the exact opposite pattern than observed in Nrf2-GFP.

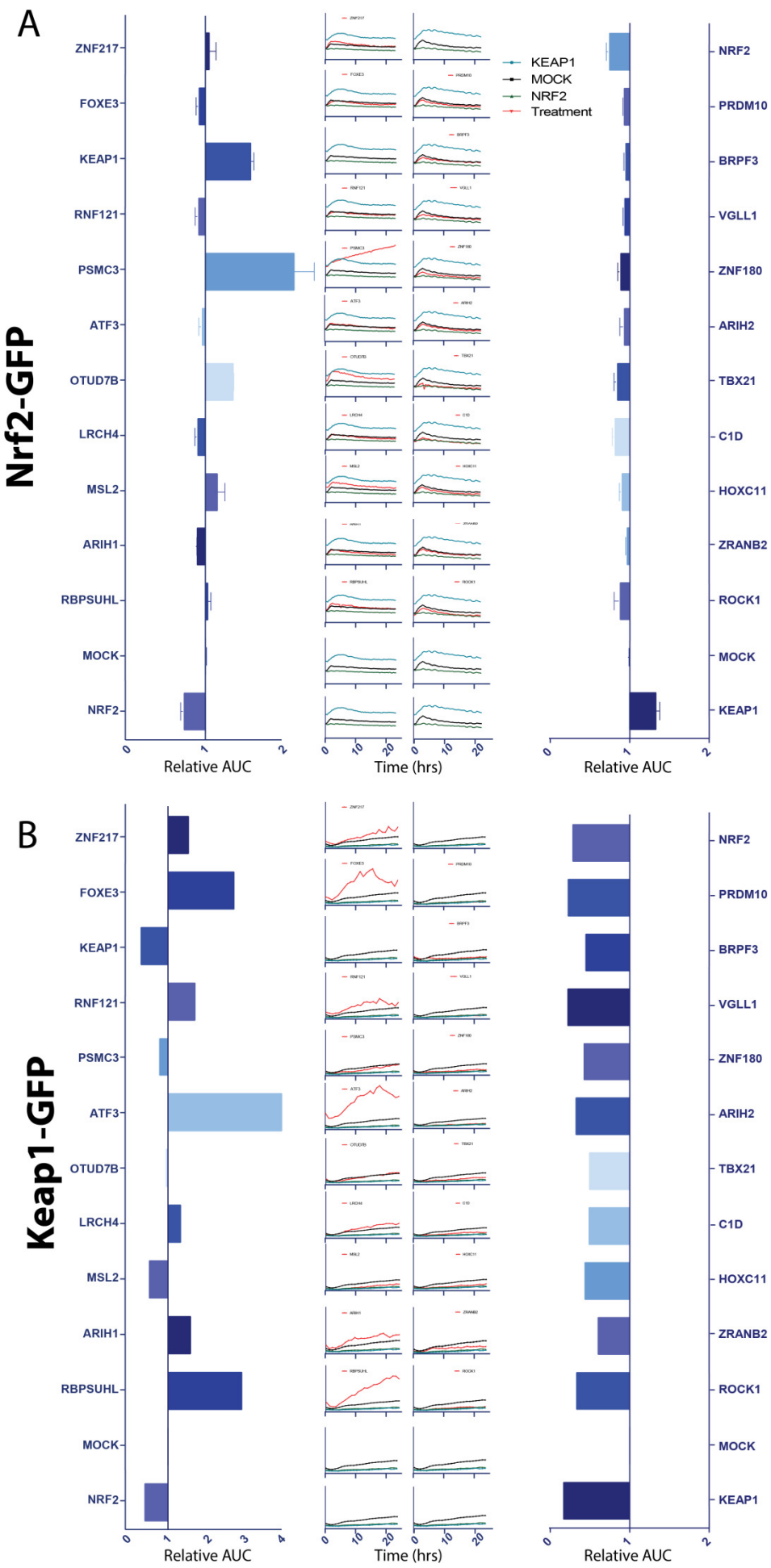

Figure 6: Ten selected hits for activation and inhibiting hits tested on Nrf2-GFP and Keap1-GFP. A) Relative GFP expression of the area under the curve of time course imaging of Nrf2-GFP after stimulation with 30 nM CDDO-me for ten selected activating hits (left) and ten selected inhibiting hits (right). 24 hour time courses are shown, with time on the x-axis and mean GFP intensity on the y-axis. siKEAP1 is depicted in blue, mock in black, siNFE2L2 in green and the hits in red. B) same as A, but for Keap1-GFP amount of foci per cell.

Knock down of positive enhancers of Nrf2 increase susceptibility to cell death

Since Nrf2 is central in the control of cytotoxicity, we hypothesized that hits inhibiting the Nrf2 response upon knock down would

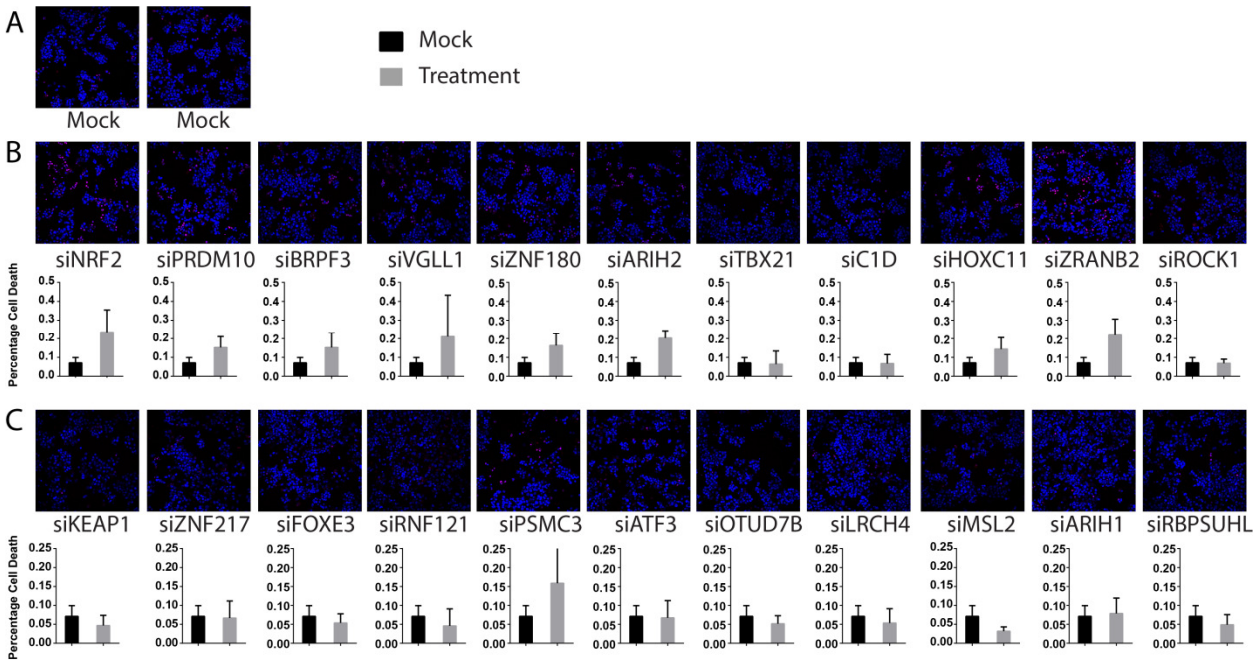

Figure 7: Increased cell death after knock down with inhibiting hits and reduced cell death after knock down with activating hits. A)Two example images of cell death staining after 1 mM 24 hours DEM. B) Example images of cell death staining after knock down with inhibiting hits (upper) and bar graph of 24 hours with mock and knock down as a mean and standard deviation of three independent replicates. All images shown are 512x512 pixels.

sensitize cells for cell death as a result of reduced protection. And, along with this hypothesis, that knock down of hits activating the Nrf2 pathway would enhance the protection and reduce cytotoxicity. Therefore, we exposed Srxn1-GFP cells to toxic concentration of 1 mM DEM (Hiemstra and Niemeijer *et al*., manuscript in preparation). We stained Srxn1-GFP cells with necrosis marker propidium iodide and apoptosis marker annexin-V-Alexa633 and subsequently measured the amount of cells stained using live cell confocal microscopy for 24 hours. We used Srxn1-GFP cells to be able to check knock down efficiency (data not shown). We observed clear increase in cytotoxicity upon knock down of Nrf2, which was not observed in knock down of Keap1. Enhancers PRDM10, BRPF3, VGLL1, ZNF180, ARIH2, HOXC11 and ZRANB2 demonstrated increased cell death staining upon DEM exposure (figure 7B). Furthermore, suppressors ZNF217, FOXE3, RNF121, ATF3, OTUD7B, MSL2 and RBPSUHL did not show an increase in cytotoxicity (figure 7C). Taken together, most enhancers are important in cytoprotection, related to Nrf2 signaling.

Discussion

In the current study we have conducted a large RNAi based screen to unravel signaling components that modulate Nrf2 activity. We validated 58 suppressors of the Nrf2 response pathway which activate Nrf2 upon knock down. If we rank these 58 hits based on induction normalized to mock after seven hours of CDDO-me exposure, we did observe three out of

twelve highest ranked hits with a known direct Nrf2 link: ATF3, BRD4 and RXRA. Activating transcription factor 3 (ATF3) is demonstrated to bind to Nrf2 and thereby inhibiting the Nrf2 binding to the ARE[218]. Bromodomain protein 4 (BRD4) causes upregulation the Nrf2 response upon stress and knock down[219]. Retinoid X receptor alpha (RXRA) is regulated by Nrf2, the induction of Nrf2 signaling upon RXRA knock down suggests a negative feedback loop[55]. These known direct links between observed hits and the Nrf2 pathway ensured us that our screening approach led us to important novel regulators of the Nrf2 pathway.

We have systematically validated 19 genes that are positive regulators of the Nrf2 pathway and, thus, which inhibit Nrf2 signaling upon knock down. None of these genes were previously associated with Nrf2, however BRPF3 (part of the MOZ/MORF complex) and FOXO4 (associated with caveolin-1) suggest that indirect links with Nrf2 signaling are present[220,221]. Knock down of all enhancers showed reduced Nrf2 activation for all assays; Srxn1-GFP, Nqo1-GFP, Keap1-GFP and Nrf2-GFP . This supports a high confidence in these novel enhancers of Nrf2 signaling.

Hmox1 is a well-studied Nrf2 target gene involved in heme catabolism. Hmox1 is regulated by Nrf2, however induction can be inhibited by transcriptional repressor Bach1[211]. Therefore, knock down of Keap1 did not induce Hmox1-GFP. Remarkably, Hmox1-GFP was reduced upon Keap1 knock down. This suggests a compensatory mechanism of Hmox1 repression by Bach1 when Keap1 is not present. In addition, CDDO-me was not able to induce Hmox1-GFP, probably because it is repressed by Bach1. In contrast, DEM was able to induce Hmox1. CDDO-me is thought to directly bind to cysteine residues on Keap1 and DEM is believed to deplete glutathione which is followed by a more general Nrf2 response. Thus, this indicates the more direct activation of Nrf2 signaling by CDDO-me compared to DEM. The fact that Hmox1 is not activated in each condition Nrf2 dissociates from Keap1 suggests that Nrf2 target gene expression is tightly regulated. Therefore, the Hmox1-GFP result delivered more mechanistic insight in how these hits are regulated. In addition, Nqo1-GFP was inducible by CDDO-me and showed reduction with the inhibiting hits upon knock down. However, less suppressors showed an effect in Nqo1-GFP. An explanation for this could be the already high basal expression of Nqo1-GFP, which is only slightly induced by compounds or knock down.

The results in Nqo1-GFP and Hmox1-GFP can be combined with Nrf2-GFP and Keap1-GFP results to give a lead in the mechanistic research for some of the individual hits. However, Keap1-GFP did not show large distinction in enhancers as knock down of these genes result in a reduction of Keap1-GFP. This is in concordance with what we already observed earlier and supports the hypothesis that increase in Keap1-GFP foci formation is dependent on Keap1 and likely p62 expression by Nrf2 (Hiemstra and Niemeijer *et al.*, manuscript in preparation). In contrast, the suppressors showed a remarkable opposite effect in Keap1-GFP compared to Nrf2-GFP. Three inducers of Nrf2 accumulation, PSMC3, OTUD7B and MSL2, inhibit Keap1-GFP foci formation. This would suggest a mechanism in which Keap1 degradation is inhibited with Nrf2 accumulates in the nucleus. Additional experiments should give a conclusion on this.

Future research will focus on unraveling the mechanism of individual hits in their role in Nrf2 activation. Based on the protein function of the candidate genes we can already suggest a role in Nrf2 activation. In basal conditions, Nrf2 is continuously targeted for proteasomal degradation by Keap1 via ubiquitination. Therefore, candidate genes from the ubiquitin family, as TRIM71 and TRIM72, might be involved in this process. Upon oxidative stress Nrf2 accumulates in the nucleus and transcribes its targets. Nrf2 is known to form heterodimers with MAFs and Bach1, suggesting candidate genes from the transcription factor family (i.e. ZNF217, FOXE3, PRDM10, ZNF180, RNF121, TBX21) are involved in Nrf2 activation in a similar way. In addition, BRPF3, a histone deacetylase could be involved in transcription of Nrf2 target genes. Furthermore, different kinases are known to be involved in phosphorylation of Nrf2, which in turn activates an Nrf2 response. Thus, candidate kinases, as ROCK1, PRPF4B and CERK could play a role in Nrf2 target activation. Lastly, different binding partners are identified interring with Nrf2 activation. Other genes like LRCH4 or RBPSUHL could be involved in a similar way. However, further research is needed to be able to pinpoint the exact role of candidate genes in Nrf2 activation.

Next to their role in Nrf2 activation individual, candidate genes can be evaluated for their role in the switch between adaptation and cell death. The onset of this insight is given in figure 7, where cells are pushed to the boundary of cytotoxicity using high concentrations of DEM, to elucidate the role of the hits in adaptation and cell death. Whether knock down of candidate genes affect cytotoxicity is important knowledge to prevent DILI. DILI only occurs in susceptible individuals, and single nucleotide polymorphisms (SNPs) in critical hepatotoxicity modulators could play a role. Possibly our candidate genes are rich in genetic polymorphisms and as such could contribute as individual risk factors for DILI. In addition, novel regulator of Nrf2 activation could also play a role in cancer, as lung cancers have mutations in Keap1 which activate Nrf2, to protect cells from cell death[222]. Likewise, our candidate genes could serve as oncogenes in certain cancers by modulating Nrf2 activity and supporting overall cellular fitness and survival.

In conclusions, we have systematically identified novel regulators of the Nrf2 stress response pathway. We appreciate that these novel regulators contribute to an improved mechanistic understaniding in DILI onset, but may also enable further understanding of mechanisms of drug resistance in cancer therapy.

Acknowledgements

This work was supported by the IMI MIP-DILI project (grant agreement number 115336); the EU FP7 Seurat-1 Detective project (grant agreement number 266838).

Supplementals

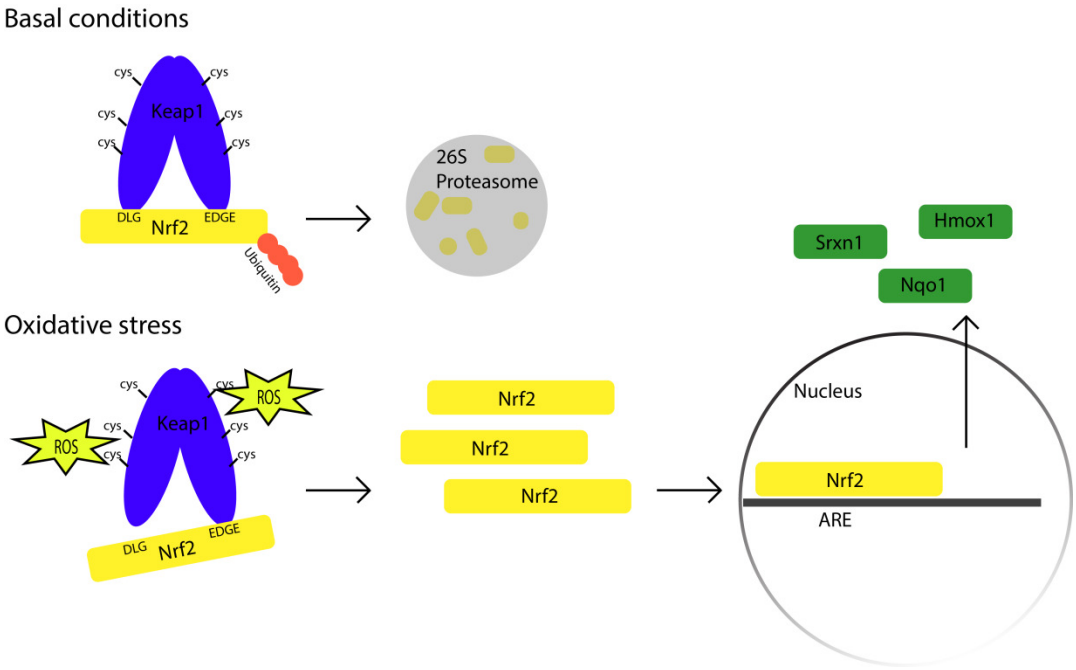

Supplemental figure 1: Nrf2 pathway activation. Under basal conditions Nrf2 is bound by Keap1, ubiquitinated and degraded. Under oxidative stress, reactive oxygen species inhibit ubiquitination of Nrf2, Nrf2 accumulates and translocates to the nucleus. Nrf2 will bind to the anti-response element and transcribe its detoxifying targets.

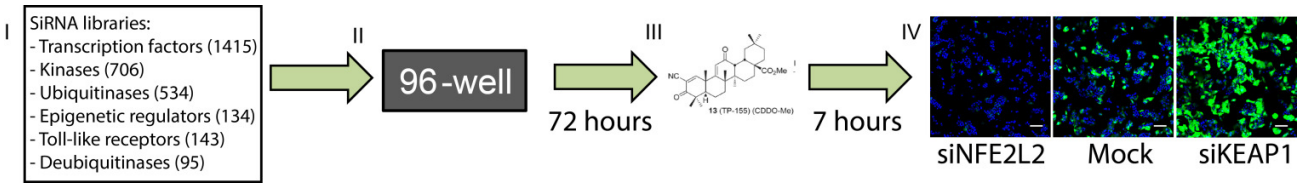

Supplemental figure 2: Screen set-up. I) siRNA library containing 3027 genes divided over different siRNA libraries were II) transfected in 96-well format III) stimulated with CDDO-me and IV) after 7 hours imaged with live confocal imaging. Scale bars represent 100 µm.

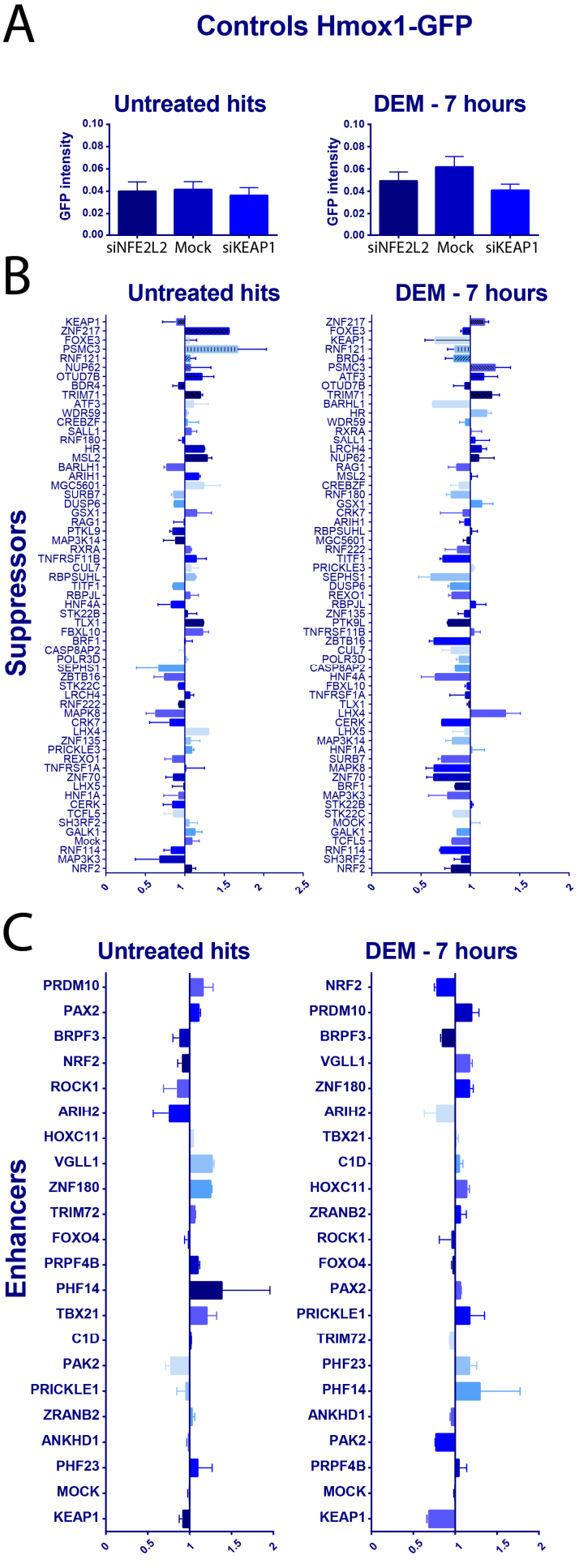

Supplementary figure 3. Effect of suppressors and enhancers on Hmox1-GFP expression. A) Mean GFP intensity of Hmox1-GFP for siNFE2L2, mock and siKEAP1 for untreated (left) and DEM 100 µM for 7 hours (right). B) Relative GFP expression of suppressors in Hmox1-GFP. C) Relative GFP expression of enhancers in Hmox1-GFP.

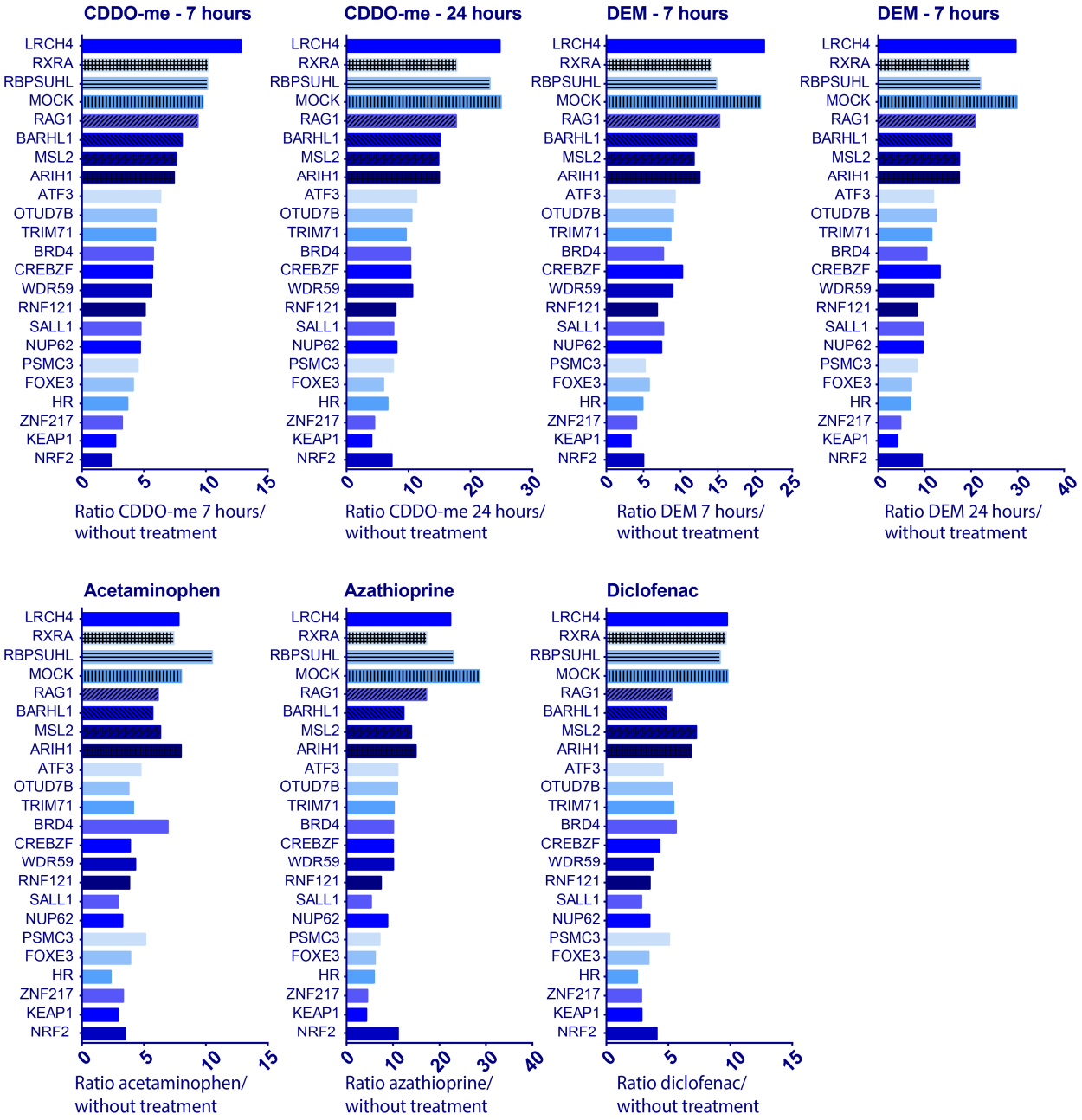

Supplemental figure 4: Ratios of compound treatment versus no compound treatment for top 20 activating hits. Ratios of compound treatment versus no compound treatment for top 20 activating hits for CDDO-me 7 and 24 hours, DEM 7 and 24 hours, acetaminophen, azathioprine and diclofenac.